INTERNATIONAL JOURNAL OF GEOMAGNETISM AND AERONOMY
VOL. 6, GI3007, doi:10.1029/2005GI000113, 2006

Modeling of the electron density profile of the lower ionosphere (45–75 km) for sudden ionospheric disturbance conditions based on the data on sudden phase anomalies of VLF signals

M. I. Belenkiy, A. B. Orlov, G. A. Petrova, and A. N. Uvarov

Physical Research Institute, St. Petersburg State University, St. Petersburg, Russia

Received 14 April 2005; revised 21 March 2006; accepted 9 August 2006; published 14 December 2006.

[1] By using a large sample of data on sudden phase anomalies (SPA) of VLF signals (frequencies 11.9 and 13.6 kHz), a model of winter and summer electron density profiles $N(h)$ of the near-noon lower ionosphere (45–75 km) for the conditions of sudden ionospheric disturbances (SIDs) has been developed. The main subject of the study has been parameter b, which characterizes the relation between the electron density N and ionization rate q. The dependencies of b on height h and latitude θ (in the interval 35°S to 55°N) have been found for summer and winter. The magnitudes of parameter b obtained by analyzing SPA have been compared with its values calculated by using a theoretical detailed model of ion chemistry of the lower ionosphere and also the global $N(h)$ model of the ionosphere for quiet conditions. Below 65 km the results are consistent. The discrepancies in the magnitudes of b occur for middle latitudes 30°–55°N, summer conditions, and heights of 70–75 km. The changes in the electron density profiles during SIDs deduced from the SPA data for these conditions are several times higher than theoretical estimates. Considerable latitudinal variations in parameter b and $N(h)$ profile during SID have been found to occur only in summer at the heights indicated above and latitudes 0°–30°N. *INDEX TERMS:* 7223 Seismology: Earthquake interaction, forecasting, and prediction; 2435 Ionosphere: Ionospheric disturbances; 0342 Atmospheric Composition and Structure: Middle atmosphere: energy deposition; *KEYWORDS:* VLF waves propagation; Lower ionosphere; Sudden ionospheric disturbances.

Citation: Belenkiy, M. I., A. B. Orlov, G. A. Petrova, and A. N. Uvarov (2006), Modeling of the electron density profile of the lower ionosphere (45–75 km) for sudden ionospheric disturbance conditions based on the data on sudden phase anomalies of VLF signals, *Int. J. Geomagn. Aeron., 6,* GI3007, doi:10.1029/2005GI000113.

1. Introduction

[2] Modeling of the electron density height distribution $N(h)$ in the lower ionosphere (heights $h < 90$ km) under quiet and disturbed conditions has been the subject of numerous research efforts. In our paper, attention is focused on analysis of regular seasonal and latitudinal variations in the characteristics of the lowest layers of the daytime ionosphere, $h < 65 - 70$ km which have been very little studied experimentally [*Smirnova and Danilov*, 1998]. Vast opportunities for the investigation of the lower ionosphere are offered by analysis of SPA of the signals in the VLF range under SID conditions [*Mitra*, 1974]. Determination of the effective electron loss coefficient ψ was one of the directions in the investigations of the D region of the lower ionosphere in the 1960s and 1970s. The computing facilities needed for performing a large volume of calculations of VLF fields based on the use of sufficiently complete and strict models of the ionosphere were not powerful enough in those years. Necessary information on physical and chemical parameters of the D region was not available as well. These factors hindered reliable estimation of ionospheric parameters from different data and, in particular, from the data on SPA [*Itkina*, 1978; *Mitra*, 1974]. In addition, the ionospheric information was obtained mainly for altitudes above 65–70 km.

[3] The investigation described in this paper was aimed at modeling of the vertical distribution of electron density $N(h)$, $h < 75$ km, for SID and quiet conditions. The object of the investigation was the effective parameter $b \approx \sqrt{1/\psi}$, which under quasi-stationary conditions establishes the rela-

1524–4423/06/2005GI000113$18.00

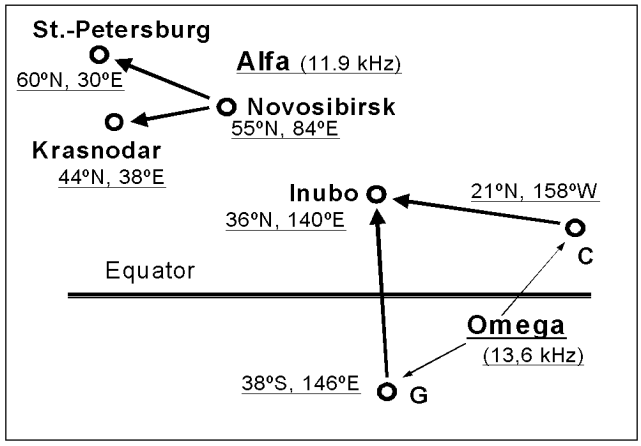

Figure 1. Scheme of the propagation paths.

tion between the electron density N and electron production rate q, $N \approx b\sqrt{q}$. Earlier, analyzing sudden phase anomalies of VLF signals, *Orlov et al.* [1998a, 1998b] estimated approximately the ψ coefficients for heights of 50–75 km, the latitudinal interval 0°–80°, and summer conditions. The goal of the investigation was also to analyze regular seasonal and latitudinal variations in parameter b for near-noon conditions by using a large sample of homogeneous data on SPA and also to compare the vertical profiles $b(h)$ obtained from the SPA data with the $b(h)$ dependencies for quiet conditions. The investigations were carried out for the latitudinal interval 35°S to 65°N.

[4] The use of vast volumes of the initial data on VLF propagation should provide a possibility to obtain reliable estimates of the space-time variations in N values in the lower ionosphere. However, such problems may be solved only attracting functional models containing relatively small number of parameters to be determined. The choice of the type of such model for parameter b is based in this paper on the results of the calculations with the help of the multicomponent ion chemistry model of the lower ionosphere by *Petrova and Kirkwood* [2000]. The final results obtained by SPA make it possible to test the theoretical model attracted.

2. Experimental Data on SPA and Method of Their Processing

[5] The statistical estimates for sudden phase anomalies presented below were obtained from measurements of phases of VLF signals for the paths (Figure 1) more than 3 Mm in length. For basic investigations, 6 samples of the SPA data (three samples for the summer and winter seasons each) were used, of which four samples formed by using Communications Research Laboratory (CRL) data (Ionospheric Data in Japan, vols. 42–48, nos. 1–12, Indep. Admin. Inst., Tokyo, 1990–1996) characterized the SPA of the signals of radio stations C and G of the Radio Navigation System (RNS) "Omega" (at a frequency of 13.6 kHz) received from 1989 to 1995 at Inubo (Japan). The lengths of the C–Inubo and G–Inubo paths were 6110 and 8230 km, respectively. In addition, experimental data on the SPA for the Novosibirsk–Krasnodar path (3300 km in length) obtained by the authors from the signals of RNS "Alfa" (a frequency of 11.9 kHz, a period of recording 2000–2002) were used.

[6] The data on SPA and sudden enhancement of signals (SES) of RNS "Alfa" (a frequency of 11.9 and 14.9 kHz) for the Novosibirsk–St. Petersburg path are considered as well. These data were also obtained in the framework of the study reported here. In addition, generalized characteristics of the SPA for the NWC–Inubo path obtained by *Orlov et al.* [1998a] from CRL data are invoked as an illustration.

[7] In the samples, the data for the time intervals from June to August and from December to February were assumed to correspond to summer and winter conditions, respectively (for the Northern Hemisphere). The solar activity level was taken into account. For the time interval considered it was characterized, on the average, by the Wolf number $W = 90$. To characterize the solar flare intensity, the X-ray emission burst magnitude Γ_8 in the 1–8 Å range at the moment of its maximum (from Solar-Geophysical Data (part 2, 1995–2002)) was used. Weak flares with the emission intensity $\Gamma_8 < (2-3) \times 10^6$ W m^{-2} were excluded from the analysis of SPA (below the subscript index 8 is omitted if it is insignificant).

[8] At the first stage of the initial data processing, the dependence of the average illumination of the paths determined by the average zenith angle of the Sun $\chi_{\rm av} = \arccos\{\overline{\cos}\chi\}$ on time UT (Figure 2) was analyzed for each sample. Here, the magnitude of $\overline{\cos}\chi$ is the value of $\cos\chi$ averaged over the illuminated part of the path defined by condition $\chi < 90°$. From the position of the minimum of the approximating dependence $\chi_{\rm av}$(UT), typical noon values of χ_n and UT$_n$ (Table 1) corresponding to the maximum illumination of the path were found for each sample of events. Therefore the estimates of the ionosphere parameters obtained from the values of UT$_n$ characterize near-noon conditions.

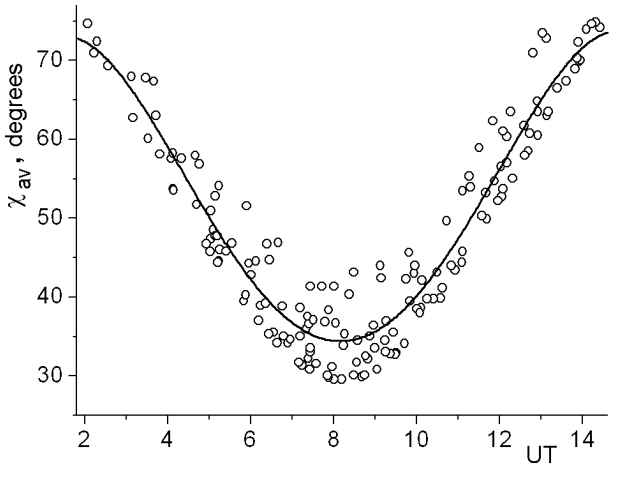

Figure 2. Dependence of the illumination of the Novosibirsk–Krasnodar path on time UT for summer ($M = 6 \div 8$).

Table 1. Results of Processing of Experimental Data on SPA $\hat{\Phi}_{ek}(\Gamma, \mathrm{UT}_n)$[a]

M	Path	V	$\hat{A}$	$\hat{B}$	$\hat{C}$	UT_n (χ_n)	$\hat{\Phi}_{ek}(\Gamma, \mathrm{UT}_n)$		
							$\Gamma = 5\times10^{-6}$	$\Gamma = 1.6\times10^{-5}$	$\Gamma = 5\times10^{-5}$
6,7,8	Nov.–Kr.	161	62.3 ± 4.2	10.8 ± 0.8	7.7 ± 2.1	0810 (34.0°)	4.5 ± 0.4	9.9 ± 0.5	15.3 ± 0.8
6,7,8	C–Inubo	85	75.9 ± 7.5	13.2 ± 1.4	8.5 ± 3.1	0024 (19.9°)	5.6 ± 0.6	12.3 ± 0.8	18.8 ± 1.4
6,7,8	G–Inubo	74	81.6 ± 6.2	14.3 ± 1.2	4.9 ± 3.3	0227 (26.3°)	5.5 ± 0.6	12.7 ± 0.7	19.8 ± 1.1
6,7,8	NWC–Inubo	59	–	–	–	0330	–	–	17.5 ± 1.6
12,1,2	G–Inubo	207	87.4 ± 4.5	15.5 ± 0.9	5.4 ± 2.4	0232 (24.3°)	4.9 ± 0.4	12.7 ± 0.5	20.4 ± 0.8
12,1,2	C–Inubo	219	98.7 ± 6.4	17.7 ± 1.3	–	0032(52.5°)	5.2 ± 0.5	14.1 ± 0.6	22.8 ± 1.1
12,1,2	Nov.–Kr.	37	93.2 ± 16	15.4 ± 2.6	15.9 ± 12	0828 (73.3°)	3.0 ± 1.5	10.8 ± 1.3	18.4 ± 2.1

[a] $\hat{A}$,$\hat{B}$, $\hat{C}$, and $\hat{\Phi}$ are given in degrees Mm^{-1}, and Γ is in W m^{-2} for the spectral window 1 – 8 Å. Here, Nov.–Kr., Novosibirsk–Krasnodar.

[9] Each sample of the data on SPA was processed with the help of the two-parameter regression model. The magnitude of SPA was determined from the decrease in phase φ_i observed during a SID at the moment of time when the phase minimum occurred. Then it was divided by the length of the illuminated part of the path R_i. The empirical dependence of $\Phi_i = \varphi_i / R_i$ on $\overline{\cos}\chi$ and X-ray radiation flux Γ was determined in the form

$$\Phi = A + B \lg \Gamma + C \lg(\overline{\cos}\chi) \quad (1)$$

Table 1 lists the number of events V in the analyzed samples and obtained estimates of regression parameters $\hat{A}$, $\hat{B}$, and $\hat{C}$ for winter (M = 12, 1, 2) and summer (M = 6, 7, 8) months.

[10] Analysis of six dependencies of transformed experimental values of $Y_i = \Phi_i - \hat{C} \lg(\overline{\cos}\chi_i)$ on the logarithm of burst intensity $\lg \Gamma_i$ revealed that these dependencies exhibit a high linearity (see the example in Figure 3). Attempts to use different more complicated dependencies, nonlinear with respect to $\lg \Gamma$ and $\lg(\overline{\cos}\chi_i)$, instead of equation (1) did not result in a more precise description of the initial samples of Φ_i. Note that coefficients $\hat{B}$ and $\hat{C}$ are close to each other only in some cases (see Table 1). Therefore the dependence of the form $\Phi = A + B' \lg \Gamma(\overline{\cos}\chi)$ used earlier by *Orlov et al.* [1998a, 1998b] is not always applicable for processing of experimental data on SPA.

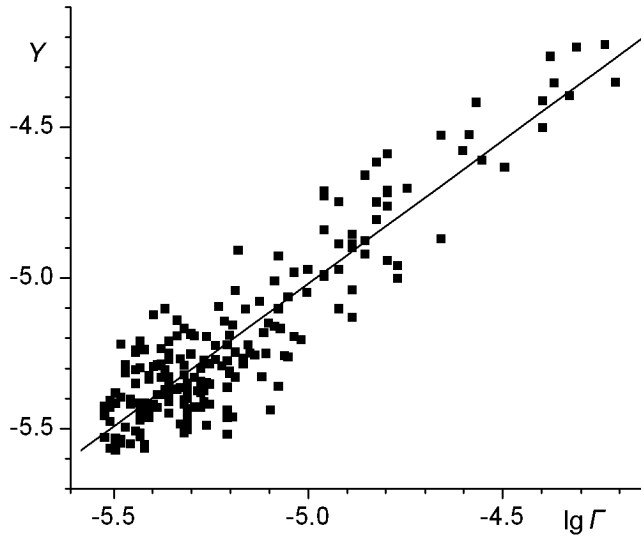

Figure 3. Dependence of normalized SPA on flare intensity (the G–Inubo path). The effect of variations in illumination is excluded.

[11] Table 1 lists experimental estimates of $\hat{\Phi}_{ek}$ obtained from approximation (1) for the magnitudes of $(\overline{\cos}\chi)_{nk}$ corresponding to the time moments UT_{nk} (the k index defines the conditional order number of the estimates of $\hat{\Phi}_{ek}$ calculated through equation (1) for different paths and levels of Γ, k = 1, 2, ..., 18) for three levels of the X-ray flux ($\Gamma = 5\times10^{-6}$, 1.6×10^{-5}, and 5×10^{-5} W m^{-2}). The use of three levels of Γ for the analysis allows one to get information on not only the slope but also the degree of nonlinearity of the $\Phi(\lg \Gamma)$ dependence. Table 1 also gives half widths of the confidence intervals $\Delta\Phi_{ek}$ (with the "±" sign) corresponding to the 95% confidence probability for the obtained estimates of $\hat{\Phi}_{ek}$. The estimates of the SPA magnitudes obtained in this way determine with a sufficiently high precision and reliability typical (but not averaged in the trivial sense) manifestations of SIDs in the VLF phase under fixed conditions. The estimates of $\hat{\Phi}_{ek}$ found for different magnitudes of Γ give information on the $N(h)$ profile in different height intervals. As Γ grows, the rigidity of the flare spectrum increases, and the lower boundary of the region in which the X-ray radiation affects the atmosphere becomes lower. For instance, under typical summer midlatitude conditions at $\Gamma = 5\times10^{-6}$ W m^{-2} the flare radiation gives rise to additional ionization only at heights above 60 km, and at the intensity equal to 5×10^{-5} W m^{-2} the region of disturbance extends to much lower heights (Figure 4). This necessitates the use of the magnitudes of SPA at different levels of Γ for the solution of the problem.

3. Model of the Electron Density Profile of the Lower Ionosphere During SIDs

[12] To analyze experimental data on SPA, we used, like *Demykin et al.* [1991] and *Orlov et al.* [1998a], the model

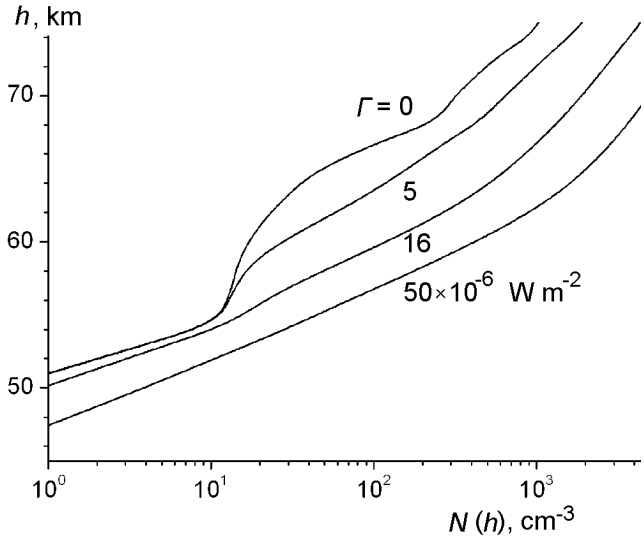

Figure 4. Summer midlatitude ($\theta = 50^\circ$) near-noon profiles of the electron concentration $N(h)$ for quiet conditions (the model [*Azarnin et al.*, 1987; *Gosstandart of Russia*, 1995]; see the text) and for SID conditions (this paper) at various intensities of solar X-ray emission bursts.

of the ionosphere during SIDs that contains three basic elements, i.e., the electron density profile $N_0(h)$ for quiet conditions on the background of which a SID occurs, the height dependence of the additional electron production rate $\Delta q(h)$ under the action of the flare electron emission, and parameter $b(h)$ that defines electron losses. In contrast to the papers mentioned above, the basic expression used here is

$$N = b \times \{q\}^s \tag{2}$$

In this empirical formula (and in what follows) N and q have dimensions cm^{-3} and s^{-1} cm^{-3}, respectively. The initial information on parameters b and s was obtained by analyzing the $N(q)$ dependencies calculated from the detailed theoretical model of ion chemistry of the lower ionosphere by *Petrova and Brunelli* [1990] and *Petrova and Kirkwood* [2000]. The power s in equation (2) is somewhat higher than 0.5. At $s = 0.5$, the value $1/b^2$ acquires the meaning of the commonly used effective loss coefficient ψ. For quiet conditions equation (2) includes N_0 and ionization rate q_0, and for SID conditions equation (2) contains $q_d = q_0 + \Delta q$, where $\Delta q = \Delta q(h)$ is the ionization rate increment. It is assumed that maximum Δq is reached at all the heights of interest simultaneously.

[13] At a height $h < h_c = 64 - 66$ km free electrons in the atmosphere under quiet conditions are produced under the action of the galactic cosmic rays (GCR), and during SIDs an additional source of ionization is the solar flare X-ray radiation. Both ionization sources exert influence on all the basic constituents of the atmosphere, and therefore equation (2) must define the relation between N and q under both quiet and SID conditions at the same magnitudes of parameters b and s ($b_0 = b_d$, $s_0 = s_d$). By using this fact, it is easy to deduce from equation (2) the formula for calculation of the electron density profile $N_\mathrm{d}(h)$ during SIDs (including quiet conditions) in the quasi-stationary approximation

$$N_\mathrm{d} = [N_0^{1/s} + b^{1/s} \times \Delta q]^s \tag{3}$$

At heights $h > h_c$, where the decisive role is played by the wave radiation of the Sun, photochemical processes in the ionosphere under quiet conditions and during SIDs are different. According to *Mitra* [1974] and *Itkina* [1978], at heights 70–75 km, even during weakest SIDs ($\Gamma \le (2 \div 3) \times 10^{-6}$ W m^{-2}), the values of b can increase by a factor of 4–6 as compared with quiet conditions. Therefore the validity of equation (3) does not raise doubts only in trivial cases, i.e., at $\Delta q \gg (N_0/b)^{1/s}$, where $b = b_d$, and at $\Delta q \to 0$. However, it should be noted that the dominant role in formation of the VLF field under SID conditions is played by the ionosphere at heights below 65 km. Therefore it can be supposed that inaccuracies of model (3) due to its use for the entire height interval, from 45 to 70–75 km, will not cause considerable errors in the final results for $N_\mathrm{d}(h)$. A final judgement on the success in solving the problem can be made on the basis of the accuracy achieved in description of the whole body of data on SPA and SES considered here.

[14] The $N_0(h)$ is taken in (3) within the height interval 45–105 km in the similar way as it has been done by *Orlov et al.* [1998a, 1998b] using the global model [*Azarnin et al.*, 1987; *Gosstandart of Russia*, 1995]. At heights above 75 km this model had been fitted with the *Rawer et al.* [1978] and *Gosstandart of Russia* [1990] models. At lower heights it is based on the data on VLF propagation. The model is analytical and describes all the principal space-time regular variations in $N(h)$ profiles in the quiet lower ionosphere: latitudinal, 11-year heliocyclic, seasonal (including the November effect), and diurnal (including the sunrise-sunset asymmetry).

[15] The value of $\Delta q(h)$ was calculated from the X-ray flux intensity Γ, geographical coordinates, number of month, and time of day in accordance with the *Orlov et al.* [1998a] model.

[16] The spectrum of the X-ray burst is described by the exponential model

$$F(\lambda) = A\lambda^{-2} \exp\left(\frac{-hc}{\lambda k T}\right)$$

where $A = \Gamma_4 \{ \int_{0.5}^{4} F(\lambda) d\lambda \}^{-1}$ is the amplitude multiplier, k is the Boltzmann constant, and T is the temperature parameter of the flare calculated by the empirical formula $T^\circ\,\mathrm{K} = 1.2 \times 10^8 (\Gamma_4^{0.17} - 0.016)$, Γ_4 [W m^{-2}] being the integral intensity of the X-ray burst within the $0.5 \div 4$ Å range. The transition from the values of the integral intensity Γ_8 [W m^{-2}] determining the intensity of the solar flare in this paper to the value of used in the previous paper by *Orlov et al.* [1998a] was performed using the empirical formula:

$$\lg \Gamma_4 = (66.6 \lg \Gamma_8 + 417.3)^{0.37} - 11$$

[17] The value of the increment of the ionization rate during SID was calculated taking into account latitude, season,

and the illumination degree using the formula based on the Chapmen ion production function [see, e.g., *Whitten and Poppoff*, 1975]. The modified and taking an approximate account for the Earth sphericity this function have the form

$$\Delta q(h,\theta,\chi,\Gamma_8) = \int_{0.5}^{11} n(h)\sigma(\lambda)AF(\lambda,\Gamma_8)W^{-1}\times$$

$$\exp\{-\sigma(\lambda)\int_{h}^{h_1} n(z)\left[1-\left(\frac{a}{a+z}\right)^2\sin^2\chi\right]^{-1/2}dz\}d\lambda$$

where h is the height over the Earth surface ($h_1 = 105$ km), a is the Earth radius, $n(h)$ is the density of the atmosphere (according to the CIRA (1972) model) depending on latitude and season, $\sigma(\lambda)$ is the cross section of the X-ray absorption [*Nicolet*, 1964], χ is the solar zenith angle and $W = 35$ eV is the energy required to form one ion-electron pair. It should be noted once more that the model for the $\Delta q(h)$ value is one dimensional because of the use of the empirical quantitative relation of its temperature parameter with the X-ray burst value Γ. The fact of the dependence of the temperature parameter of the flare (or its hardness degree of its spectrum) on its intensity has been numerously noted *Mitra* [1974].

[18] Thus the model of the electron density profile $N_\mathrm{d}(h, x_k, d_m, \Gamma)$ for SID conditions was built on the basis of equation (3). Parameters x_k characterize the conditions to which the $N_\mathrm{d}(h)$ profile corresponds, and parameters d_m enter the model of the effective parameter $b = b(h,\theta,d_m)$ and determine its height and latitudinal variations. The model of the b parameter was the main object of the investigations reported in this paper, and parameters d_m were to be determined.

4. Model of the Effective Parameter *b*

[19] The functional form of the model $b = b(h,\theta,d_m)$ was at first chosen on the basis of literature data [*Orlov et al.*, 1998a] and then refined by using the results of approximation of the $N(q)$ dependencies calculated from the detailed model of ion chemistry of the lower ionosphere suggested by *Petrova and Brunelli* [1990]. In a later paper, *Petrova and Kirkwood* [2000] listed all the processes included into this model with their constants and also literature sources from which they were taken. The model includes approximately 150 reactions with participation of 19 species of positive ions and 17 species of negative ions, photodetachment of electrons from negative ions and photodissociation of positive and negative ions, dissociative recombination of electrons and positive ions, and also mutual neutralization of ions of both signs. A large volume of literature data on the processes in the lower ionosphere in which charged particles participate was analyzed, and the set of the most important reactions and their rates was specified [*Petrova and Brunelli*, 1990]. Preference was given to the results obtained by laboratory measurements. Particular emphasis was placed on taking into account the temperature dependencies of the decomposition reaction rates of complex ion clusters (in the region from 300 to 200 K). The problem of the determination of equilibrium concentrations was solved by numerical integration of the system composed of the continuity equations for all the species contained in the model (electrons included).

[20] The model described above was used in our investigations to analyze ionization of the atmosphere by galactic cosmic rays and X-ray flare radiation of the Sun. In view of this fact, the specified rate of additional ionization Δq was distributed between two basic ions in the proportion $q(\mathrm{O}_2^+) = 0.9\Delta q$ and $q(\mathrm{NO}^+) = 0.1\Delta q$ [*Swider*, 1979]. Therefore the numerical results obtained by using this model characterize the processes of electron formation at heights below 65 km under quiet and SID conditions, and above 65 km the results are valid for SID conditions. Note that in this paper because of the unavailability of the necessary data on the height distribution of concentrations of minor neutral constituents during SIDs, the data for the quiet midlatitude conditions were used in the model.

[21] Approximation of the theoretical $N(q)$ dependencies was performed in a sufficiently wide interval of variations Δq which included the magnitudes of q typical for quiet conditions and SIDs with an X-ray flux of up to $\Gamma = 5\times10^{-5}$ W m^{-2} for all the heights analyzed. The dependencies of N on q for fixed h were approximated by a power function in the form of equation (2). As a result, the $b(h)$ and $s(h)$ dependencies for latitudes 0 and 50° qualitatively similar to those derived earlier by *Petrova* [1986] for PCA conditions were obtained. For both the summer and winter conditions, parameter s in the height interval 54–80 km varies in an irregular fashion in the range 0.5–0.58 and becomes equal to 1 at a height of 50 km. Therefore, in all the investigations the $s(h)$ dependence was taken to be $s = 0.55$ for $h > 54$ km, $s = 1$ for $h < 50$ km, and a linear interpolation was used for the interval 50–54 km. The use of the magnitudes of $s(h)$ given above had to make the model dependence $N_\mathrm{d} = N_\mathrm{d}(\Gamma)$ more close to the class of dependencies following from the theoretical model.

[22] In all the cases considered, the dependence of parameter b on height (Figure 5, TM curves) at heights below 60 km and above 65 km can be regarded as nearly exponential, with appreciably differing gradients. It can be described in the entire height interval, from 45 to 75 km, as

$$b(h) = A_0\{A_1(\theta)\exp[g_1(h-H)]+$$

$$A_2(\theta)\exp[g_2(h-H)]\}^{-1} \quad (4)$$

where $g_1 = -0.325$ km^{-1}, $g_2 = -0.04$ km^{-1}, $H = 62$ km, $A_{1,2}$ are the multipliers which depend on latitude θ, and A_0 is a fixed scaling multiplier. The value of $2g_2$ is in satisfactory agreement with a gradient of -0.06 km^{-1} in the $\psi(h)$ dependence taken from *Azarnin et al.* [1997]. Using the experimental data on SPA [*Orlov et al.*, 1998b], the gradient of the $\psi(h)$ dependence for heights below 60 km was refined; the obtained value of -0.6 km^{-1} nearly coincides with the magnitude of $2g_1$. In the vicinity of the height H, a changeover of the dominating role of the first and the second exponents in equation (4) occurs. This feature of the

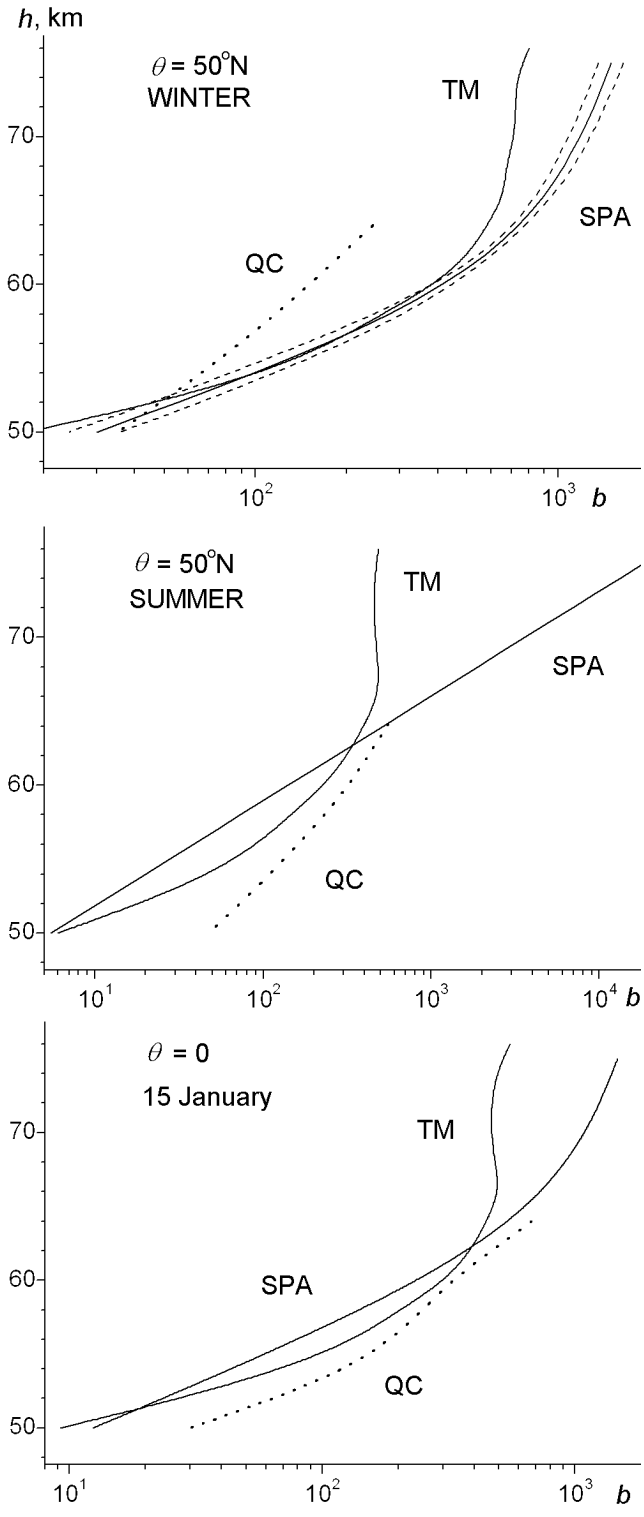

Figure 5. Dependencies $b(h)$ for winter and summer middle-latitude conditions and also for the equator (January) inferred from analysis of sudden phase anomalies (SPA curves), calculated from the theoretical photochemical model (TM curves), and obtained from height profiles $N_0(h)$ for quiet conditions (QC curves).

$b(h)$ dependence agrees well with the form of the $\psi(h)$ dependencies in summer models [*Orlov et al.*, 1998a, 1998b]. Parameter A_0 was estimated by *Azarnin et al.* [1997] for summer conditions from the VLF data during SID and PCA events to be $A_0 = 426$.

[23] The data on SPA for paths with different latitudinal positions described above do not allow one to reveal any details of the latitudinal dependencies $A_{1,2}(\theta)$ with a spatial scale less than 20°–30°. For this reason, a simplest representation was used for these dependencies

$$\lg A_1 = d_1 + d_{2,4}|\theta - d_{11}| + d_{3,5}(\theta - d_{11})^2$$

$$\lg A_2 = d_6 + d_{7,9}|\theta - d_{11}| + d_{8,10}(\theta - d_{11})^2 \qquad (5)$$

In the expressions given above, θ is the geographical latitude ($\theta > 0$ in the Northern Hemisphere), d_{1-5} and d_{6-10} are the parameters that characterize latitudinal variations of exponents with gradients g_1 and g_2, respectively, parameters $d_{2,3,7,8}$ determine winter dependencies, and parameters $d_{4,5,9,10}$ are related to summer dependencies. Calculations were performed for the Northern Hemisphere winter (for 15 January) and summer (for 15 July). It was supposed that equal values of parameter b for 15 January and 15 July (formally this implies the absence of seasonal "winter–summer" variation) can occur at latitude $\theta = d_{11}$ different from the equator. It was assumed that latitudinal variations in $b(\theta)$ to the north of latitude $\theta = d_{11}$ in January are identical to those in July to the south of the same latitude (this statement remains valid in the case of a 6-month shift). Thus initially the model contained 11 free parameters that had to be determined. The authors also studied other forms of height and latitudinal dependencies. The model presented in this paper was chosen as a result of the search for the description of the height and latitudinal dependencies that would eventually lead to a reasonable compromise between simplicity of the model (with a minimum number of parameters) and accuracy of description of the initial body of data.

5. Estimation of the Parameters of the Model b (h, θ, d_m)

[24] By using the $N_{\rm d}(h, x_k, d_m, \Gamma)$ model described above and height dependencies for the effective collision frequency of electrons and neutral particles [*Azarnin et al.*, 1987], normalized values of SPA $\Phi_{\rm mod} = \Phi_{\rm mod}(h, x_k, d_m, \Gamma_k)$, $k = 1, 2, ..., K$; $K = 18$ were calculated for the paths analyzed and conditions considered. At time moments UT_n (Table 1), all the paths were fully illuminated. The VLF field at long propagation paths was calculated by the method of normal waves. In the calculations, the nonhomogeneity of the propagation paths caused by changes in the properties of the terrestrial surface and anisotropic ionosphere was taken into account (that is, taking into account variations in all parameters of the waveguide channel along the propagation path) [*Galuk and Ivanov*, 1978]. The effects of normal waves transformations were not taken into account in the calculations

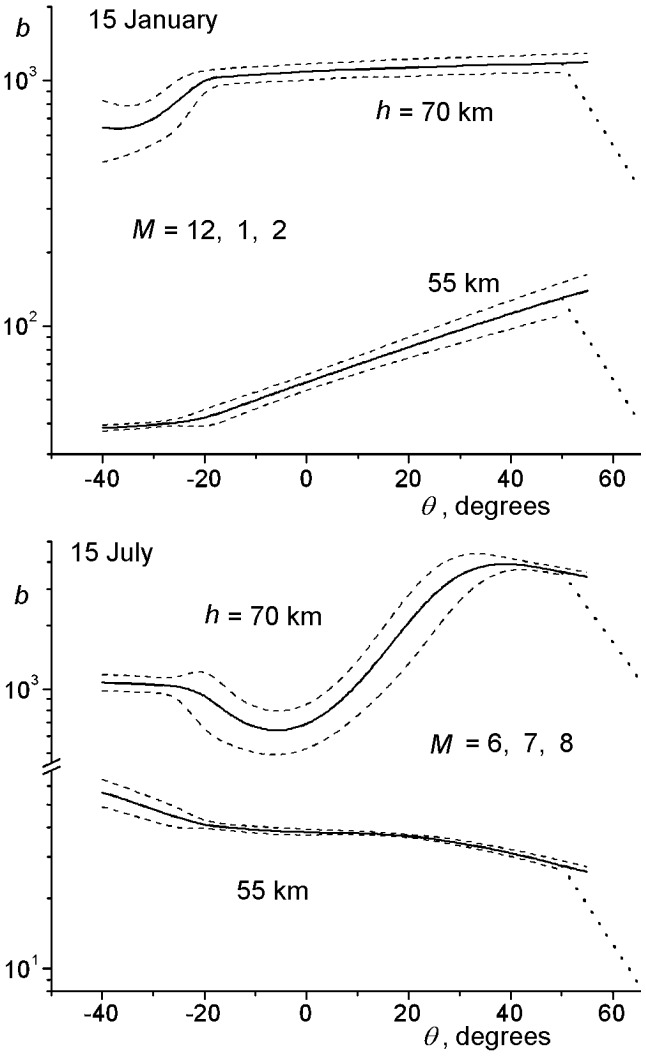

Figure 6. Parameter b as a function of latitude for two heights. It is calculated for 15 January and 15 July from the model suggested in this paper. The curves are not shown outside the interval 35°S to 65°N because experimental data for these latitudes are not available. The dashed curves mark the confidence interval for the 95% significance level.

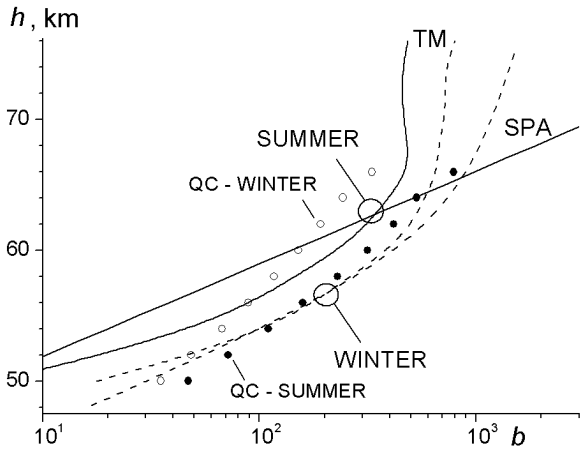

Figure 7. Seasonal variations of the $b(h)$ profile for the latitude 50°N.

because of the absence at the propagation paths parts with considerable changes in the properties of the ionosphere and Earth surface (that is, the WKB approximation was used). The accuracy of the phase of the VLF field was considerably higher (by an order of magnitude or more) than the accuracy of the experimental data.

[25] The estimates of parameters $\hat{d}_m$ determining the unknown for $b(h,\theta)$ dependencies were obtained by the least squares method from the condition of minimum of the sum

$$S = \sum_{k=1}^{K} \frac{\left[\Phi_{\mathrm{mod}}(h, x_k, d_m, \Gamma_k) - \hat{\Phi}_{ek}\right]^2}{(\Delta\Phi_{ek})^2} \qquad (6)$$

the accuracy of experimental estimates of $\hat{\Phi}_{ek}$ being taken into account. The minimum was found by the coordinate descent method. Of the set of 11 estimates of $\hat{d}_m$, only the significant ones were used for the final solution. The null hypothesis for the parameter $\hat{d}_m$ ($\hat{d}_m = 0$) was rejected if after exclusion of this parameter the criteria statistics $\hat{F} = (S_{(P-1)} - S_P)(K-P)/S_P$ (where S_P and $S_{(P-1)}$ are the magnitudes of the sum S after minimization using P and $(P-1)$ parameters) fell into the upper region of the Fisher distribution $F\,(1, K-P)$ at a significance level of 5% [*Draper and Smith*, 1966]. In addition, the situations when two and three parameters were excluded were analyzed. Estimates of six significant parameters $\hat{d}_m$ at which S goes to a minimum $S_{\min} = 1.31$ are given in Table 2.

[26] Confidence intervals for estimation of parameters $\hat{d}_m$ and subsequently of $\hat{b}$ were determined by two methods using linearization of the $\Phi_{\mathrm{mod}}(h, x_k, d_m, \Gamma_i)$ function in the region of the minimum: (i) from the obtained value of $S_{\min}$, by using a standard scheme of the least squares method; and (ii) by the method of error transfer of the initial data (the covariance matrix for $\hat{\Phi}_{ek}$ was taken into account). The root-mean-square error for residual normalized discrepancies in sum (6) was sufficiently low, about 0.3. This fact and also the approximate equality of the estimates of errors in b obtained by the two methods indicated that systematic errors due to inadequacy of the $N_{\mathrm{d}}(h)$ model relative to the initial data did not give a significant contribution into $S_{\min}$. Because of the smallness of residual differences in equation (6), the model values $\Phi_{\mathrm{mod}}(h, x_k, \hat{d}_m, \Gamma_i)$ are not given in Table 1.

[27] The set of the estimates of $\hat{d}_m$ (Table 2) was an immediate result of the investigation. It determined the optimal estimates of the $N_{\mathrm{d}}(h,\Gamma)$ profiles during SIDs. However, from the physical point of view a consideration of the $b(h,\theta)$ dependencies (Figures 5–7) is interesting. Examples of the height and latitudinal dependencies of the b parameter are shown in Figures 5 and 7 and Figure 6, respectively. The confidence interval for the parameter b calculated for the confidence probability 95% varies, depending on conditions, mainly from ±3% to ±15%. An example of the accuracy "band" for the winter dependence $b(h)$ is shown in Figure 5. The b parameter is estimated with higher accuracy at alti-

Table 2. Significant Estimates of Parameters d_m Minimizing Functional (6)

Parameter	Valued
d_2, rad^{-1}	−0.456
d_5, rad^{-2}	0.129
d_6	−0.327
d_9, rad^{-1}	1.84
d_{10}, rad^{-2}	−3.45
d_{11}, rad	−0.37

tudes of 60–65 km, whereas the largest errors (up to ±20%) take place in winter at latitudes 30°–55°N in the lower part of the considered height interval $h = 45 - 50$ km. The latter fact is due to the decrease at these heights of the value of Δq because of relatively large value of χ. Moreover, the accuracy decreases considerably (down to 25–50%) in summer at heights of 70–75 km in the vicinity of $\theta = 30°$N.

[28] It follows from the latitudinal dependencies $b(\theta)$ shown in Figure 6 that the most significant variations occur in summer conditions at latitudes of 0°–30°N. The seasonal variations of b are such that at a latitude of 50°N the winter values of the parameter b at heights below 60 km exceed the summer values by a factor of 3–5 (Figure 7, the curves with the index SPA). At a height 65 km the seasonal variation change sign and increases with an increase of h.

[29] The obtained dependencies $b(h, \theta, \hat{d}_m)$ characterize some typical properties of the lower ionosphere. The estimates of b values are obtained in the class of functions determined by expressions (3) and (4) for the considered conglomerate of geophysical conditions, in particular for the latitudinal interval from 35°S to 55°N. The accuracy bands shown in Figures 5 and 6 (dashed curves) determine the regions where there can be collated only realizations of the $b(h, \theta)$ dependencies belonging to the chosen class of functions. Moreover, naturally, the obtained results characterize the ionosphere only within the height region where the ionosphere governs propagation of VLF signals of the considered frequencies in the waveguide channel "the Earth–ionosphere." In the solved problem this region is located at altitudes from 45–50 km to 70–75 km.

6. Additional Analysis of SES and SPA Effects

[30] In order to additionally test the developed SID model, sudden enhancement of signals (SES) at a frequency of 11.9 kHz observed for the Novosibirsk–St. Petersburg path (3100 km) was analyzed for summer and winter periods of 1999–2001. The onset of a SID leads to a slight sudden enhancement of signals, i.e., the SES effect, in the overwhelming majority of cases. The magnitude of the enhancement characterizes the maximum deviation of the amplitude from its undisturbed value. Below it is given in percent. As compared with SPA, the SES formation exhibits a number of distinguishing features. At a SID maximum, an increase in the phase velocity of the dominating normal wave (with the lowest number) is almost always observed, and the argument of its excitation coefficient remains nearly unaltered regardless of the magnitude of Γ and changes in the spectrum shape of an X-ray burst. As a consequence, the phase of the far nearly one-mode field decreases, and the SPA effect takes place. Simultaneously, the attenuation rate and modulus of the excitation coefficient of the normal wave increase. While the first factor reduces the field strength, the second factor leads to its increase. The magnitude of the detected net SES effect appreciably depends on the signal frequency, length of the propagation path and its other characteristics, and also on specificity of changes in the $N_d(h)$ profile whose shape is determined by the spectral characteristics of each particular X-ray emission burst. Therefore, while the values of SPA correlate well with the flare intensity Γ, no such correlation is observed for SES.

[31] Figure 8 shows experimental magnitudes of SES and calculated dependencies of SES on flux Γ. In forming the experimental sample, the zenith angle of the Sun was not taken into account, however, the propagation path had to be fully illuminated. The calculations were performed for noon by using the latitudinal model (5) modified by taking into account the results of *Orlov et al.* [1998a, 1998b]. According to them, it was assumed for the conditions of the experiment that

$$\lg A_{1,2}^{(m)} = \lg A_{1,2}(\theta) \quad \text{for } \theta \le \theta_m$$

$$\lg A_{1,2}^{(m)} = \lg A_{1,2}(\theta) + \frac{\theta - \theta_m}{\Delta\theta} \quad \text{for } \theta > \theta_m \tag{7}$$

where $\theta_m = 50°$N and $\Delta\theta = 30°$.

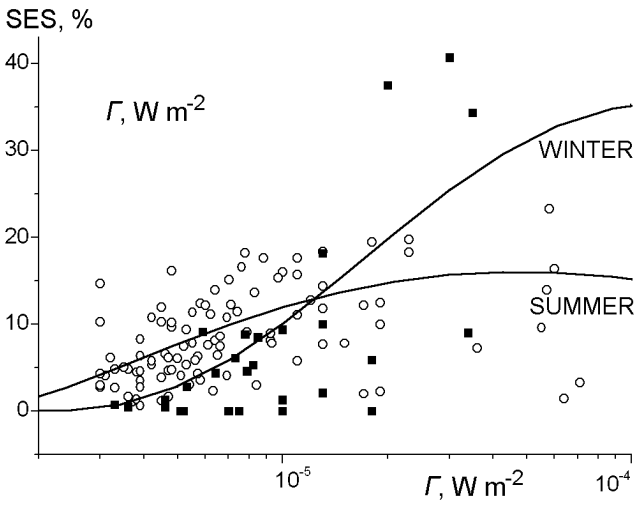

Figure 8. Comparison of calculated dependencies of SES on flare intensity with experimental SES effects for the Novosibirsk–St. Petersburg path (summer values are shown by circles, winter values are shown by solid squares, and the solid curves are calculated from the model of $N_d(h, \Gamma)$ built on the basis of SPA data).

[32] The modification (7) in the $b(\theta)$ dependence is shown in Figure 6 by dashed curves. In spite of a large scatter in the experimental data, it can be seen that at low burst levels, $\Gamma = (3-10) \times 10^{-6}$ W m^{-2}, summer values exceed winter ones, while at $\Gamma = (1-5) \times 10^{-5}$ W m^{-2} the situation is opposite. In a qualitative sense, a similar regularity is observed in the theoretical dependencies what are in satisfactory quantitative agreement with the arrays of summer and winter experimental results presented in Figure 8.

[33] With illustrative purposes, calculations for the conditions of observation of SPA of the signals of radio station NWC received at Inubo (the path length is 6960 km, frequency is 22.3 kHz, period of recording is from 1992 to 1994) were also carried out. The theoretical value calculated from the developed $N_{\rm d}(h, \hat{d}_m, \Gamma)$ model differs from the experimental value of *Azarnin et al.* [1997] given in Table 1 in the limits of accuracy of its determination

$$|\Phi_{\rm mod}(h, x_k, \hat{d}_m, \Gamma) - \hat{\Phi}_{\rm NWC}| \approx \Delta\Phi_{\rm NWC}$$

7. Analysis and Discussion of Results

[34] 1. The G–Inubo propagation path is almost symmetric with respect to the geographical equator, and therefore at $d_{11} = 0$ residual differences $\delta\Phi_{Gk} = [\Phi_{\rm mod}(h, x_k, \hat{d}_m, \Gamma_k) - \hat{\Phi}_e k]$ in equation (6) for two seasons analyzed must be equal (with an accuracy to random variations) for each of the three levels of Γ. However, when the problem was being solved with this magnitude of d_{11}, residual normalized values $\delta\Phi_{Gk}$ in equation (6) were persistently characterized by the magnitudes $\delta\Phi_{Gi} = +(0.8-1.5)$ for months 12–2 and $\delta\Phi_{Gi} = -(0.8-1.5)$ for months 6–8 for all the three levels of Γ at all the attempts to modify model (3)–(5). If these deviations are regarded as nonrandom, they can be reduced only by increasing b for one season and decreasing it for the other season in the entire interval of latitudes, from 35°S to 38°N (the latitudes of station G and receiving point at Inubo, respectively). Naturally, it is impossible to establish any details of the latitudinal dependence (with dimensions less than 20°–30°) in the equatorial belt of the latitudes considered on the basis of the materials used. One of the simplest ways to realize the required change is to introduce a shift of d_{11}. In this way an asymmetry of the latitudinal location of the propagation path relative to latitude $\theta = d_{11}$ is achieved, and the model acquires the degrees of freedom for a considerable decrease in residual errors for the six summands of sum (5) associated with the G–Inubo path. The solution yielded $d_{11} = 21.2°$S.

[35] 2. As a result of the investigation, the values of parameter b for the conditions when additional ionization caused by solar flare X-ray radiation leads to sudden phase anomalies of VLF signals, $b = b_{\rm SPA}$ (SPA curves in Figures 5 and 7), have been found in the context of model (3), (4). Under quiet conditions at heights below 62–65 km, an ionizing agent is galactic cosmic rays (GCR), $b = b_0 = b_{\rm GCR}$ and, as noted above, $b_{\rm GCR}$ must be equal to $b_{\rm SPA}$. The values of $b_{\rm GCR}$ at these heights (QC curves in Figures 5 and 7) can be calculated by using the $N_0(h)$ profiles [*Azarnin et al.*, 1987; *Gosstandart of Russia*, 1995] built on the basis of the data on VLF propagation under quiet conditions and the known rates of ionization $q_{\rm GCR}$ by galactic cosmic rays. For the calculations, exponential approximation of the $q_{\rm GCR}(h)$ dependencies given by *Rishbeth and Garriott* [1969] and *Velinov et al.* [1974] was used. It has the form

$$q_{\rm GCR} = q_0 \times \exp[g_0(h - h_0)]$$

where $g_0 = -0.13$ km^{-1}, $h_0 = 60$ km, and the magnitudes of q_0 are listed in Table 3.

Table 3. Magnitudes of Parameter qo for Different Quiet Conditions at a High Solar Activity Level, $W \approx 100$ [a]

	q_0 Value	
$\theta = 0$		0.07
$\theta = 50°$	Summer	0.043
$\theta = 50°$	Winter	0.043

[a] Parameter q_0 is electron production rate at a height of 60 km and is given in cm^{-3} s^{-1}.

[36] It is of interest to compare the values of $b_{\rm GCR}$ with the results obtained in our work for $b_{\rm SPA}$ and also with $b_{\rm TM}$ calculated from the theoretical photochemical model of *Petrova and Brunelli* [1990].

[37] It follows from Figure 5 that under the conditions considered, at heights 58–65 km, the values being compared are, on the whole, close to each other, and the discrepancies do not exceed, on the average, ±20% (with the exception of the QC dependence for winter quiet conditions). It is at these heights that the accuracy of building the $N(h)$ models from the data on VLF propagation under both quiet and disturbed conditions must be the highest. At lower heights, the discrepancy between the results increases because of higher inaccuracies of the methods and also because the QC ($N_0(h)$ profile) and SPA (this work) dependencies being compared were obtained by using different methods and functional representations.

[38] 3. The seasonal changes calculated with the help of the theoretical model have the same sign as the changes found from the SPA, but have the amplitude by a factor of 2–3 less than the latter (Figure 7). The vertical profiles $b_{\rm GCR}(h)$ found from the $N_0(h)$ profiles for quiet conditions, though look on the whole as the $b_{\rm SPA}(h)$ and $b_{\rm TM}(h)$ dependencies, however the seasonal changes of the value of $b_{\rm GCR}$ at heights 50–60 km have the opposite sign. The latter fact is significant since the most reliably determined value is the seasonal variation. This comment concerns all three results on $b_{\rm SPA}(h)$, $b_{\rm GCR}(h)$, and $b_{\rm TM}(h)$. In relation to this, one should note that the coefficients $b_{\rm SPA}(h)$ and $b_{\rm TM}(h)$ should well characterize the processes of production and loss of free electrons. Unlike these coefficients, the value of $b_{\rm GCR}(h)$ calculated from the $N_0(h)$ profiles should be determined by the vertical profile of the conductivity of the ionospheric plasma, the latter having both the electron and ion components. The found disagreement between the results requires a special study.

[39] 4. At heights 62–64 km, the middle-latitude values of $b_{\rm SPA}(h)$ and $b_{\rm TM}(h)$ are close to each other and change

only slightly on transition from winter to summer. Above these heights, $h > 65$ km, a relative similarity between the $b_{\rm SPA}(h)$ and $b_{\rm TM}(h)$ dependencies (with an accuracy to a factor of $\approx 2-3$) is observed only for winter middle-latitude and equatorial conditions (Figure 5). These facts and also the results for $b(\theta)$ shown in Figure 6 can be regarded as indirect evidence pointing to a relatively weak dependence of parameter b on the degree of disturbance of the medium during SIDs for months $M = 12$, 1, 2 at latitudes from 35°S to 65°N and for $M = 6$, 7, 8 at latitudes from 35°S to 10°N. For summer conditions and latitudes $\theta > 25° - 30°$N, at heights 70–75 km, the magnitudes of $b_{\rm SPA}$ exceed those of $b_{\rm TM}$ by a factor of 8–30. For the case $b_0 \neq b_d$, equation (3) acquires the form

$$N_{\rm d} = \left[N_0^{1/s} \left(\frac{b_d}{b_0} \right)^{1/s} + b_d^{1/s} \Delta q \right]^s$$

where $b_d = b_d(\Delta q)$. The $N_{\rm d}(h)$ profile for the SPA conditions is obtained in our work without any considerable errors, in particular, for heights 65–75 km because it is just this profile that is fitted to the initial data on SPA for different levels of Γ. As noted above, according to *Mitra* [1974] and *Itkina* [1978], $b_d/b_0 \approx 4 - 6$. Therefore it can be concluded that the b_d/b_0 ratio obtained in our work is somewhat overestimated, and hence the result $b_d/b_0 \approx 8 - 30$ is in a qualitative agreement with the literature data given above.

[40] Thus the obtained results suggest that under SID conditions the increase in the summer middle-latitude values of b_d as compared with quiet conditions is much more considerable than under equatorial and winter midlatitude conditions.

[41] This feature may be related to lower values of the temperatures in summer at $h > 65$ km. Because of this the role of the atomic oxygen increases because its concentration should increase with a growth of disturbances during SID. It is worth remembering that in the calculations with the *Petrova and Kirkwood* [2000] model, we used the concentrations of minor constituents for quiet midlatitude conditions. That is why the theoretical value of $b_{\rm TM}$ calculated at the chosen initial physical and chemical parameters of the medium at heights $h = 70 - 75$ km is small and does not describe the observed increase in N in SID conditions, especially in summer.

[42] It should be emphasized in conclusion that all the initial models used and the results compared have been obtained independently, during different time periods, by significantly differing techniques, and by different initial data. Therefore, in spite of the discrepancies in the results noted above, the comparative analysis has shown, on the whole, that the models for heights below 65–70 km describe real ionosphere parameters with a reasonable adequacy and the models for heights above 70 km and above need to be corrected.

References

Azarnin, G. V., V. A. Kolsanov, and A. B. Orlov (1987), On a plausible structure of the global model of the lower ionosphere for VLF prognosis, *Probl. Diffr. Propag. Waves* (in Russian), *21,* 112.

Azarnin, G. V., A. B. Orlov, A. E. Pronin, S. N. Sokolov, A. N. Uvarov, and Yu. V. Shtennikov (1997), Prediction of VLF fields at solar-proton events, sudden ionospheric disturbances, and during after-storm periods, *Probl. Diffr. Propag. Waves* (in Russian), *27,* 77.

Demykin, C. M., B. G. Kashin, and V. P. Kyschuk (1991), Modeling and diagnostics of VLF-signals anomaly, X-rays flux and electron density in *D* region under SID, in *The Low Frequency Earth-Ionosphere Waveguide* (in Russian), p. 22, Gylym, Alma Ata, Kazakhstan.

Draper, N. R., and H. Smith (1966), *Applied Regression Analysis,* 392 pp., John Wiley, Hoboken, N. J.

Galuk, J. P., and V. I. Ivanov (1978), Determination of characteristics of VLF fields propagation in the waveguide the Earth–ionosphere: Vertically inhomogeneous anisotropic ionosphere, in *Probl. Diffr. Propag. Waves* (in Russian), 16, p. 148, Nauka, Moscow.

Gosstandart of Russia, (1990), *Terrestrial ionosphere: Model of global distribution of density, temperature, and effective collision frequency of electrons, GOST R 25645.146-89, part 1* (in Russian), 3656 pp., Gosstandart of Russia, Moscow.

Gosstandart of Russia, (1995), *Lower ionosphere of the Earth: The model of global distribution of density and effective collision frequency of electrons for low frequency radiowave prognosis, GOST R 25645.157-94* (in Russian), 380 pp., Gosstandart of Russia, Moscow.

Itkina, M. A. (1978), Electron loss coefficient in the *D* region of the ionosphere, *Radiophysics* (in Russian), *21*(6), 777.

Mitra, A. P. (1974), *Ionospheric Effects of Solar Flares,* Springer, New York.

Nicolet, M. (1964), *Aeronomy* (in Russian), Mir, Moscow.

Orlov, A. B., A. E. Pronin, and A. N. Uvarov (1998a), Latitude dependence of the effective electron loss coefficient in the daytime lower ionosphere from the data on variations in the phase of VLF fields and riometer absorption during SID, *Geomagn. Aeron.* (in Russian), *38,* 102.

Orlov, A. B., A. E. Pronin, and A. N. Uvarov (1998b), Modeling of the effects of sudden ionospheric disturbances in the lower ionosphere from the data on VLF propagation, *Electromagnetic Waves and Electronic Systems* (in Russian), *3,* 26.

Petrova, G. A. (1986), Dependence of electron density on ionization rate, in *Investigation of the High-Latitude Ionosphere* (in Russian), p. 16, Kola Sci. Cent. of the USSR AS, Apatity, Russia.

Petrova, G. A., and B. E. Brunelli (1990), *The model of ion chemistry of the D region of the ionosphere, Preprint 90-09-77* (in Russian), 48 pp., Polar Geophys. Inst., Apatity, Russia.

Petrova, G. A., and S. Kirkwood (2000), Modeling of the electron density profile in the lower ionosphere of high latitudes, *Proc. Moscow State Tech. Univ.* (in Russian), *3*(1), 115.

Rawer, K., S. Ramakrishan, and D. Bilitza (1978), *International Reference Ionosphere, URSI special report,* 75 pp., Union Radio Sci. Int., Brussels.

Rishbeth, H., and O. K. Garriott (1969), *Introduction to Ionospheric Physics,* Elsevier, New York.

Smirnova, N. V., and A. D. Danilov (1998), Solar activity effects in the *D* region of ionosphere, *Geomagn. Aeron.* (in Russian), *38,* 92.

Swider, W. (1979), Ion production in the *D* region, *Solar-Terr. Predict. Proc., 4,* 599.

Velinov, P., G. Nestorov, and L. Dorman (1974), *Cosmic-Ray Influence on the Ionosphere and on Radio-Wave Propagation* (in Russian), Bulg. Acad. of Sci., Sofia.

Whitten, R. C., and I. G. Poppoff (1975), *Fundamentals of Aeronomy,* John Wiley, Hoboken, N. J.

M. I. Belenkiy, A. B. Orlov, G. A. Petrova, and A. N. Uvarov, Institute of Radio Physics, St. Petersburg State University, 1/1 Ul'yanovskaya Str., St. Petersburg, Petrodvoretz 198504, Russia. (ABOrlov@niirf.spbu.ru)